



Evolution of miRNA-Binding Sites and Regulatory Networks in Cichlids

Tarang K. Mehta ^{1,*} Luca Penso-Dolfin² Will Nash¹ Sushmita Roy^{3,4,5} Federica Di-Palma^{6,7} and Wilfried Haerty ^{1,6}

¹Regulatory and Systems Genomics, Earlham Institute (EI), Norwich, UK

²Bioinformatics Department, Silence Therapeutics GmbH, Robert-Rössle-Straße 10, Germany

³Department of Biostatistics and Medical Informatics, UW Madison, Madison, WI, USA

⁴Roy Lab, Wisconsin Institute for Discovery (WID), Madison, WI, USA

⁵Department of Computer Sciences, UW Madison, Madison, WI, USA

⁶School of Biological Sciences, University of East Anglia, Norwich, UK

⁷Research and Innovation, Genome British Columbia, Vancouver, Canada

*Corresponding author: E-mail: Tarang.Mehta@earlham.ac.uk.

Associate editor: John Parsch

Abstract

The divergence of regulatory regions and gene regulatory network (GRN) rewiring is a key driver of cichlid phenotypic diversity. However, the contribution of miRNA-binding site turnover has yet to be linked to GRN evolution across cichlids. Here, we extend our previous studies by analyzing the selective constraints driving evolution of miRNA and transcription factor (TF)-binding sites of target genes, to infer instances of cichlid GRN rewiring associated with regulatory binding site turnover. Comparative analyses identified increased species-specific networks that are functionally associated to traits of cichlid phenotypic diversity. The evolutionary rewiring is associated with differential models of miRNA- and TF-binding site turnover, driven by a high proportion of fast-evolving polymorphic sites in adaptive trait genes compared with subsets of random genes. Positive selection acting upon discrete mutations in these regulatory regions is likely to be an important mechanism in rewiring GRNs in rapidly radiating cichlids. Regulatory variants of functionally associated miRNA- and TF-binding sites of visual opsin genes differentially segregate according to phylogeny and ecology of Lake Malawi species, identifying both rewired, for example, clade-specific and conserved network motifs of adaptive trait associated GRNs. Our approach revealed several novel candidate regulators, regulatory regions, and three-node motifs across cichlid genomes with previously reported associations to known adaptive evolutionary traits.

Key words: miRNA, gene regulatory network, cichlid, molecular evolution.

Introduction

The molecular “tinkering” of ancestral systems and divergence of gene regulatory processes are a hallmark of evolution, and have long been thought to be associated with morphologic diversity (Wilson et al. 1974; King and Wilson 1975; Prager and Wilson 1975; Jacob 1977). Based on these theories, a number of studies have focused on gene regulatory networks (GRNs) with the aim of relating gene expression variation to phenotypic divergence (Carroll 2000, 2008; Peter and Davidson 2011). With this aim, we recently developed an integrative approach to comparatively study GRN evolution across multiple tissues along a phylogeny (Mehta et al. 2021). However, our previous approach largely focused on gene co-expression and transcription factor (TF)-binding site (TFBS) evolution, without assessing the contribution of other regulatory mechanisms toward GRN evolution, like posttranscriptional

repression. This process generally occurs at the three prime untranslated region (3'-UTR) of a gene, which can contain binding sites for both RNA-binding proteins and small non-coding RNAs (ncRNAs), such as microRNAs (miRNAs). miRNAs are key regulators of gene expression, and therefore fundamental to the evolution of novel phenotypes across the animal kingdom (Berezikov 2011).

Vertebrate clades differ dramatically in species richness, and ray-finned fishes represent the largest radiation of any group (>32,000 species). Among this radiation, the East African cichlids are a diverse clade that arguably represents the most speciose example of adaptive radiations. In the three great lakes of East Africa (Tanganyika, Victoria, and Malawi) and within the last 10 My (Genner et al. 2007; Wagner et al. 2012), one or a few ancestral lineages of cichlid fish have independently radiated into over 2,000 species. These species have been able to explore a variety of ecologic niches and partly as a result (Wagner et al.

© The Author(s) 2022. Published by Oxford University Press on behalf of Society for Molecular Biology and Evolution.

This is an Open Access article distributed under the terms of the Creative Commons Attribution License (<https://creativecommons.org/licenses/by/4.0/>), which permits unrestricted reuse, distribution, and reproduction in any medium, provided the original work is properly cited.

Open Access

2012), and have given rise to an explosive diversity of phenotypic traits (Kocher 2004). Using genome and transcriptome sequences of five representative East African species, we previously demonstrated that a number of molecular mechanisms may have contributed to diversification, including the rapid evolution of regulatory elements and the emergence of novel miRNAs that may alter gene expression programs (Brawand et al. 2014). Recent studies, focused on genomic analysis of a wider range of lake species, identified low levels (0.1–0.25%) of genetic diversity between Lake Malawi species pairs (Malinsky et al. 2018), and link species richness in Lake Tanganyika tribes to variable heterozygosity, but not to the accelerated evolution of coding sequences (Ronco et al. 2021). Investigations of Lake Victoria species have also highlighted the role of ancient indel polymorphisms in noncoding regions toward species ecologic divergence (McGee et al. 2020). These findings largely report that the genomes are very similar within same lake species. This implies that discrete differences, like regulatory changes, are likely to have an important role in controlling gene expression and function, ultimately contributing to the large phenotypic differences among species. Indeed, our comparative approach focused on the integration of gene co-expression and TFBS motifs in promoter regions, to characterize GRN evolution in six tissues of five East African cichlids (Mehta et al. 2021). We identified GRN changes along the phylogeny, including cases of network rewiring for visual genes (Mehta et al. 2021). We experimentally validated that TFBS mutations have disrupted regulatory edges across species, and segregate according to lake species phylogeny and ecology (Mehta et al. 2021). These findings suggested that GRN rewiring could be a key contributor to cichlid phenotypic diversity (Mehta et al. 2021).

By using similar techniques to those applied to study TFs (Thompson et al. 2015), previous studies in cichlids have only focused on mRNA/miRNA expression and sequence evolution at miRNA-binding sites. Previous analyses reported signatures of purifying selection on cichlid miRNA-binding sites (Franchini et al. 2016; Kautt et al. 2020), and that on average, cichlid 3'-UTRs were longer with more miRNA targets per gene than in noncichlid teleost species (Xiong et al. 2018). Conserved miRNAs tend to differ across species in their expression levels, sequence, distribution, and number of predicted binding sites (Xiong et al. 2019). Additionally, there is also evidence for the acquisition of between 36 and 1,738 novel miRNAs in the rapidly radiating cichlids (Brawand et al. 2014; Franchini et al. 2016, 2019; Xiong et al. 2019) and for a higher evolutionary rate of 3'-UTR divergence among cichlid species (Xiong et al. 2018). Genes of the longest and most rapidly evolving 3'-UTRs were found to be associated with translation and ribosomal pathways (Xiong et al. 2018).

No previous studies have analyzed the selective constraint of miRNAs and their targets in cichlids. This can be assessed by studying the turnover of miRNA-binding

sites, which can be defined as the rate at which an ancestrally conserved miRNAs acquire novel binding sites or lose existing ones along a phylogeny. Previous studies in other organisms identified more targets for older, than younger miRNAs in *Drosophila* (Nozawa et al. 2016), conserved regulatory roles for conserved miRNAs in primates (Simkin et al. 2014), and three characteristic rates of target site gain and loss during mammalian evolution (Simkin et al. 2020).

Despite the role of miRNAs as key gene regulators, the dynamic turnover of their binding sites in vertebrates (Simkin et al. 2014, 2020), and the potential role of GRN rewiring as a key contributor to East African cichlid phenotypic diversity (Mehta et al. 2021), no previous study has explored the contribution of miRNAs and miRNA-binding site turnover toward GRN rewiring events across cichlids. Instead, our previous work characterized a single layer (transcriptional activation) of cichlid GRNs solely based on gene co-expression data and predicted gene promoter TFBS interactions (Mehta et al. 2021). In this study, we use our previously published genomic data sets (Brawand et al. 2014) and predicted GRNs in five East African cichlids (Mehta et al. 2021), with the aims of (1) extending the cichlid GRNs with an additional layer (posttranscriptional repression) based on predicted miRNA-mRNA interactions; (2) integrate and analyze nucleotide conservation and/or variation at miRNA-binding sites to better understand the selective constraints driving their evolution; (3) characterize co-regulation of target genes (TGs) by TFs and miRNAs as three-node motifs to study wider GRN evolution; (4) infer instances of three-node motif and GRN rewiring attributed to regulatory binding site turnover; and (5) analyze the plausibility of whether TFBS and miRNA-binding site turnover could be associated with traits of cichlid phenotypic diversity.

Results

miRNA-Binding Site Prediction in 3'-UTRs of Genes

Building upon our previously characterized cichlid GRNs based on TFBSs (Mehta et al. 2021), and to specifically assess miRNA-binding site turnover on GRN rewiring and ultimately contributions toward cichlid phenotypic diversity, we used 992 cichlid miRNA mature sequences from 172 families (Brawand et al. 2014) to predict miRNA-binding sites in five cichlid species using TargetsScan7 (Agarwal et al. 2015). To predict high-confidence miRNA targets, we used the TargetsScan7 context++ model for miRNA targeting efficacy (Agarwal et al. 2015). Using a weighted context++ score threshold of < -0.1 (see Materials and Methods), like that previously applied in other studies of vertebrate miRNA-binding sites (Warnefors et al. 2017; Hu et al. 2019; Sayed and Park 2020), we predicted 19,613,903 miRNA-binding sites in the 3'-UTRs of 21,871 orthogroups across five cichlid species (see Materials and Methods, fig. 1A). We further filtered our data to only include 3'-UTRs from 18,799 co-expressed orthogroups to match our previous data set for downstream analyses (Mehta et al. 2021), resulting in a total of 15,390,993 predicted binding sites across the five species (fig. 1A, supplementary fig. S1, Supplementary

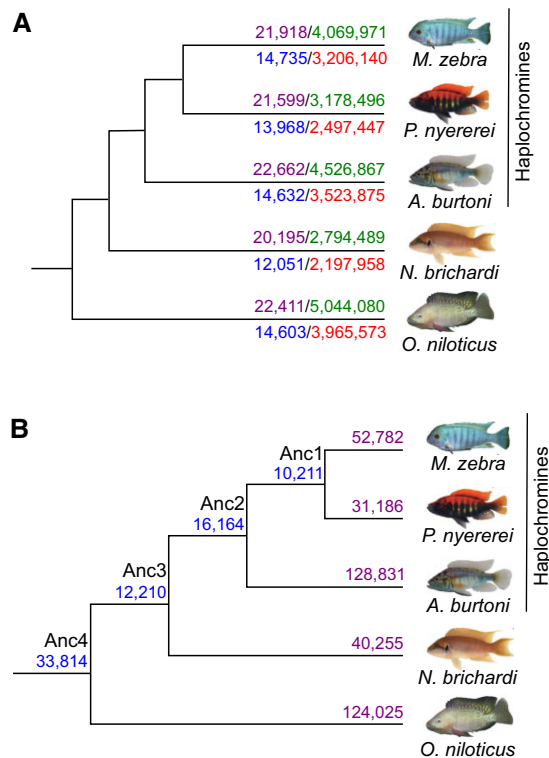


FIG. 1. miRNA target prediction in five cichlid species. (A) Number of miRNA-binding sites predicted across 3'-UTR sequences in each species. Number of all input orthogroup 3'-UTR sequences for each species (purple numbers, above branch to left) and predicted miRNA-binding sites from TargetScan7 after filtering for low quality predictions (green numbers, above branch to right) are shown for each species above the branch. Number of 3'-UTR sequences across 18,799 co-expressed orthogroups for each species (blue numbers, below branch to left) and predicted miRNA-binding sites (red numbers, below branch to right) are shown for each species below the branch. (B) Number of common and unique miRNA-binding sites across 3'-UTR sequences of co-expressed orthogroups. Number of common miRNA target sites across 3'-UTR sequences of 18,799 co-expressed orthogroups are shown at ancestral nodes and unique binding sites in each species. Common and unique binding sites at each node are defined based on overlap of unique miRNA family and target gene edges between species (see [supplementary information, Supplementary Material](#) online).

[Material](#) online). Using these predicted binding sites, we classified unique predicted miRNA-binding sites of a TG 3'-UTR as a miRNA:TG edge in each species, and compared the total number of common and unique miRNA-binding sites across all orthologous TGs based on miRNA:TG overlap (fig. 1B, see [supplementary information, Supplementary Material](#) online). We note that there are 33,814 common sites between all species and that the three haplochromine species share the second most number (16,164) of binding sites (fig. 1B). Unbiased by genome completeness or annotation quality (see [supplementary information, Supplementary Material](#) online), between 31,186 (*Pundamilia nyererei*) and 128,831 (*Astatotilapia burtoni*) unique binding sites were found to be unique to a species (fig. 1B). In total, 3'-UTR-binding sites are predicted for 172 miRNA families (*Maylandia zebra*: 118; *P. nyererei*:117; *A. burtoni*: 151; *Neolamprologus brichardi*: 115; and *Oreochromis niloticus*: 129). For instance,

miR-15c-binding sites are under-represented in *N. brichardi* ([supplementary fig. S2, Supplementary Material](#) online). This could be attributed to mutations of the *miR-15c* seed sequence in *N. brichardi* (AGCAGCG) when compared with the other species (AGCAGCA; see [supplementary information, Supplementary Material](#) online). Gene ontology (GO) enrichment of TGs for the miRNA families highlight terms that are both common, for example, membrane and signal transduction, and unique, for example, ATP binding and zinc ion binding (false discovery rate [FDR] < 0.05) between the five species ([supplementary fig. S3, Supplementary Material](#) online). Overall, variation in the number of binding sites and GO enrichment of the 172 miRNA families across the five species support differential targeting of genes in each species.

Differential miRNA-Binding Site Usage Highlights Rewiring at the Posttranscriptional Level

To study miRNA-binding site usage, we assess binding site conservation and divergence based on overlap of aligned 3'-UTR regions ([supplementary fig. S4, Supplementary Material](#) online). If at the same or overlapping positions in the alignment, a binding site has been predicted for more than one miRNA family between at least two species, then the ancestral binding site is predicted to be functionally diverged (see [supplementary information and supplementary fig. S4, Supplementary Material](#) online). Compared with an average nucleotide identity of 95–99.7% across coding sequences, representative of genomic regions under strong selective pressure, the average nucleotide identity across all 3'-UTR alignments ranges from 83% to 95% across all pairwise species comparisons. This is similar to the average nucleotide identity of 85–89% across pairwise comparisons of each species whole genome, representative of the average selective pressure across all genomic regions. By filtering targets based on complete positional overlap in at least two species, we retained a total of 1,626,489 3'-UTR-binding sites across all species (18,626/18,799 orthogroups represented). To predict functional divergence, we classified unique predicted miRNA-binding sites of a TG 3'-UTR as a miRNA:TG edge in each species, and assessed the number of shared sites (in orthologous TGs) utilized by miRNA families that are either the same (miRNA:TG overlap; fig. 2A, [supplementary fig. S5a, Supplementary Material](#) online) or different (no miRNA but only TG overlap; fig. 2B, [supplementary fig. S5b, Supplementary Material](#) online) between species. Consistent with the previous findings (fig. 1B), most sites (50,212) are conserved across all species (Anc4 node, fig. 2A). Following the phylogenetic relationships, the haplochromine species share the second highest number (Anc2 node: 32,087) of binding sites (fig. 2A). Overall, binding sites are generally conserved and utilized by orthologous miRNA families along the whole phylogeny. Counter to this, compared with basal phylogenetic comparisons (Anc4:1 and Anc3:17 shared sites), there is more miRNA family divergence within the haplochromine lineage (Anc2:3163 and Anc1:3200 shared sites; fig. 2B). For

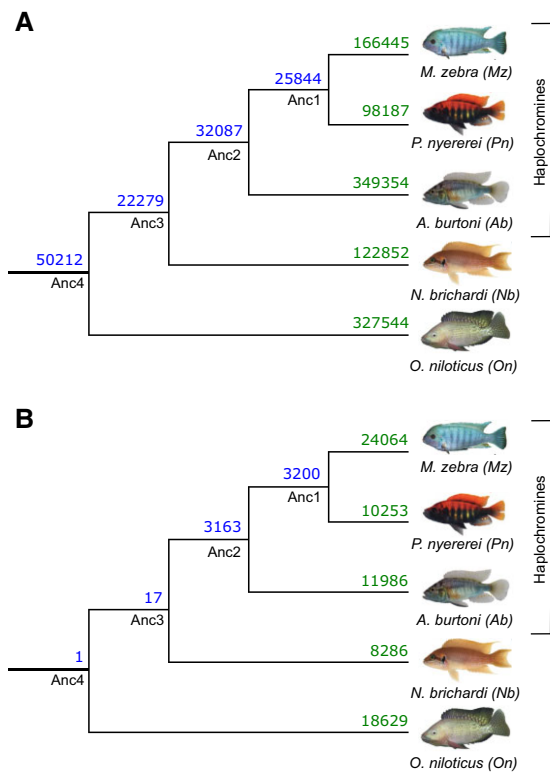


Fig. 2. Evolution of miRNA-binding sites along the five cichlid phylogeny. Number of shared and non-shared target sites based on miRNA-binding site overlap in multiple 3'-UTR alignments are shown at ancestral nodes and branches for (A) same miRNA families and (B) different miRNA families.

example, the developmental gene, *gata6*, has one miRNA-binding site (*miR-27d*) shared between *N. brichardi* and *O. niloticus*, but in the haplochromines, has three miRNA-binding sites (*miR-219*, *miR-128*, and *miR-27*).

Comparative Analysis of Three-Node Motifs Identifies Increased Novel Network Architecture between the Five Cichlid Species

As a GRN can be composed of both transcriptional activation and posttranscriptional repression, we extend our previous analysis of cichlid GRN evolution (Mehta et al. 2021) by instead focusing on “three-node motifs” (Alon 2007). As previously shown for mammals (Stergachis et al. 2014), the study of such motifs may serve as a reliable indicator of evolutionary conserved and diverged network signatures across species. Owing to the input data set and our aim of focusing on the impact of miRNA-associated GRN rewiring in five cichlids, we focus on a topology representative of a miRNA feed-forward loop (miRNA-FFL; fig. 3A). In this model, the TF is predicted to regulate a TG and a miRNA is predicted to directly regulate either the TF or TG (fig. 3A). According to this model and to avoid any bias of gene/miRNA loss or mis-annotations in motif/binding site comparisons across all species, we filtered a starting set of 37,320,950 three-node motif edges (supplementary fig. S6, Supplementary

Material online) for 1-to-1 orthologous TFs, TGs, and miRNA families. This resulted in a final set of 17,987,294 three-node motif edges across the five species (see supplementary information and supplementary fig. S7, Supplementary Material online). In this set, 467,279 (3%) three-node motif edges are conserved across all five species (supplementary fig. S8 and table S2, Supplementary Material online). Instead, 1,321,875 (7%)–3,124,263 (17%) three-node motifs are unique to each species (supplementary fig. S8 and table S2, Supplementary Material online). In the 17,987,294 three-node motif edges, we identified 429,197 (TF:TG) and 366,302 miRNA:TG unique edges across the five species. Using the presence and absence matrices of these unique edges, we note that on average, 56% of miRNA:TG edges are lost compared with 46% of all TF:TG edges across five species (see supplementary information and supplementary fig. S9, Supplementary Material online).

Using the same unique edges of each TG, we identified 115,031 unique TF:miRNA relationships and assessed their frequency to identify co-regulatory conservation and divergence along the phylogeny (see Materials and Methods). Of these TF:miRNA relationships, 25,209 (22%) are conserved across all five species. An example

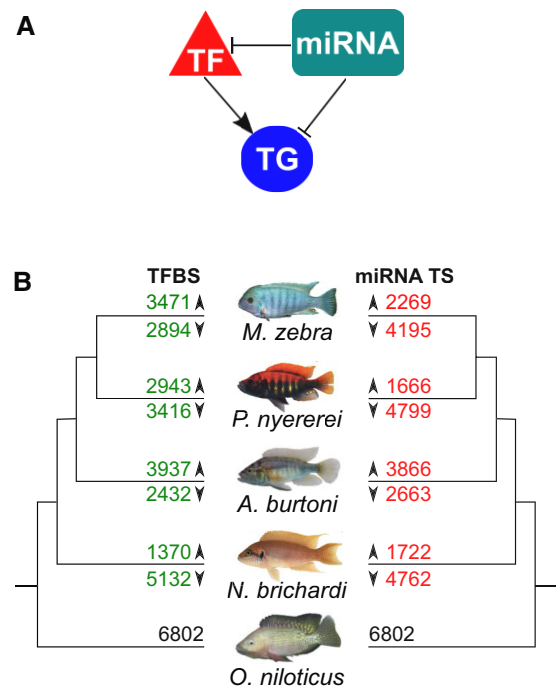


Fig. 3. Evolution of three-node motifs (transcription factor [TF]-target gene [TG]-miRNA) in cichlids. (A) Three-node motif model used to assess network architecture. The three-node motif model used is representative of a miRNA feed-forward loop (miRNA-FFL). (B) TFBS and miRNA target site gain and loss in edges of 1-to-1 orthologous target genes in three-node motifs of four cichlids. Five cichlid phylogeny showing number of 1-to-1 target gene orthologs with either TFBS (to left) or miRNA (to right) gain (above branch) or loss (below branch) versus *O. niloticus*. Binding sites in *O. niloticus* were used as reference for calculating gains and losses in the other species for 1-to-1 orthogroups.

of one such conserved relationship is *miR-18*, a miRNA with negatively correlated expression with mRNA pairs in Midas cichlids (Franchini et al. 2019), being paired with NR2C2, a TF that we previously implicated in visual opsin GRN rewiring in cichlids (Mehta et al. 2021). On the other hand, 35,137 (31%) TF:miRNA relationships are unique to any one species and target an average of 5,658 genes across the five species, of which, 25 out of the 90 genes associated with phenotypic diversity from previous studies are also targeted (see [supplementary information](#) and [supplementary table S3, Supplementary Material](#) online). For example, *fgfr1*, a gene implicated in shaping cichlid scales (Albertson et al. 2018), is a species-specific target in *A. burtoni* of 48 co-regulatory relationships, for example, KLF5B:*miR-27e*; and IRF7:*miR-27b* is a unique co-regulatory relationship of *M. zebra*, and targets the fast-evolving (Brawand et al. 2014) morphogenesis gene, *bmpr1* (see [supplementary information](#) and [supplementary fig. S10, Supplementary Material](#) online). Overall, by looking at three-node motifs, we identify evolutionary conserved signatures as well as much more novel species-specific network architecture that can be associated with traits of cichlid phenotypic diversity.

Network Rewiring is Associated with Different Models of Regulatory Binding Site Turnover in Three-Node Motifs Across Species

The previous section focused on the evolution of whole network motifs. Here, we determine whether species differences in edges of these motifs are due to regulatory binding site turnover associated with previously described GRN rewiring events (Mehta et al. 2021). Using the unique TF:TG (429,197) and miRNA:TG (366,302) edges of 6,802 1-to-1 TG orthogroups, we note variation in TFBS or miRNA-binding site gain or loss along the phylogeny ([fig. 3B](#)). In the haplochromines, both *M. zebra* (4,195) and *P. nyererei* (4,799) have more TGs with miRNA-binding site losses, whereas in *A. burtoni*, there are more TGs with either TFBS (3,937) or miRNA (3,866) gain ([fig. 3B](#)). On the other hand, *N. brichardi* has more TGs (5,132) with TFBS and miRNA-binding site loss ([fig. 3B](#)).

We then sought to test the impact of miRNA-binding site turnover in the three-node motifs and characterize the model of binding site evolution. It also provides us with the opportunity to assess the relative contributions of miRNA-binding site and TFBS turnover to previously observed GRN rewiring events (Mehta et al. 2021). We previously measured rewiring rates of TFBSs (Mehta et al. 2021) using DyNet (Goenawan et al. 2016), whereby the variance of nodes and TF–TG edges in orthologous gene networks is calculated, and a rewiring metric score (degree-corrected D_n score) is outputted (Goenawan et al. 2016). After ordering the D_n score, calculating the mean for all orthogroups, and testing the significance of difference around the mean, a degree-corrected D_n score >0.17 was characterized as a threshold for significant GRN rewiring (Mehta et al. 2021). To test the associations

of GRN rewiring and binding site turnover, we use and extend our analyses in [figure 3B](#) whereby *O. niloticus* 1-to-1 orthologous genes are used as a reference to assign each of the other species genes to one of eight models of binding site evolution, including all combinations of TFBS/miRNA gain, loss, or “no change.” We then tested the significance of enrichment (hypergeometric P -value <0.05) of orthogroups in each model of binding site evolution that could be contributing to either 6,542 significantly rewired (degree-corrected D_n score >0.17) or 260 low to nonrewired (degree-corrected D_n score ≤ 0.17) 1-to-1 orthogroups (see Materials and Methods). We report that TFBS gain/loss (mean degree-corrected D_n score = 0.21), instead of miRNA-binding site gain/loss (mean degree-corrected D_n score = 0.20), had the largest effect on significantly rewired (degree-corrected D_n score >0.17) orthologs ([fig. 4A, supplementary fig. S11, Supplementary Material](#) online). The most associated models of rewired orthologs are TFBS loss in *A. burtoni* ($P = 0.009$) and TFBS gain in *M. zebra*, *P. nyererei*, and *N. brichardi* ($P = 0.0007$ – 0.03 ; [supplementary table S5, Supplementary Material](#) online). However, all low to nonrewired orthologs (D_n score ≤ 0.17) that should be impervious to TFBS-based rewiring are expectedly most associated with no change in TFBS, but miRNA-binding site loss in all four species ($P = 0.000005$ – 0.05 ; [supplementary table S6, Supplementary Material](#) online). This therefore indicates a discrete impact of GRN rewiring based on miRNA-binding site loss. Overall, this suggests that different models of regulatory binding site evolution have impacted GRN rewiring in the studied cichlid lineages.

Regulatory Binding Site Turnover in Three-Node Motifs is Associated with Network Rewiring of Adaptive Trait Genes

Further examination of the rewired orthologs with either of the eight models of binding site evolution identifies teleost and cichlid trait genes associated with phenotypic diversity from previous studies ([fig. 4B, supplementary information, supplementary fig. S13, and table S3, Supplementary Material](#) online). Compared with all orthologs (mean D_n rewiring score = 0.17), we previously showed that four visual opsin genes (*sws1*, *rho*, *sws2a*, and *rh2b*) have considerably rewired networks (D_n score = 0.23–0.28) in species utilizing the same wavelength visual palette and opsin genes (Mehta et al. 2021). The evolution of GRNs and utilization of diverse palettes of co-expressed opsins is able to induce shifts in adaptive spectral sensitivity of adult cichlids (Carleton 2009). Such quantitative and qualitative changes of opsin gene expression can fine-tune cichlid vision in response to prey, ambient light changes, or even conspecific signals and is thought to be primarily achieved through differential regulation (Hofmann et al. 2009; O’Quin et al. 2012). In this respect, we previously demonstrated that opsin expression diversity could be the result of TF regulatory

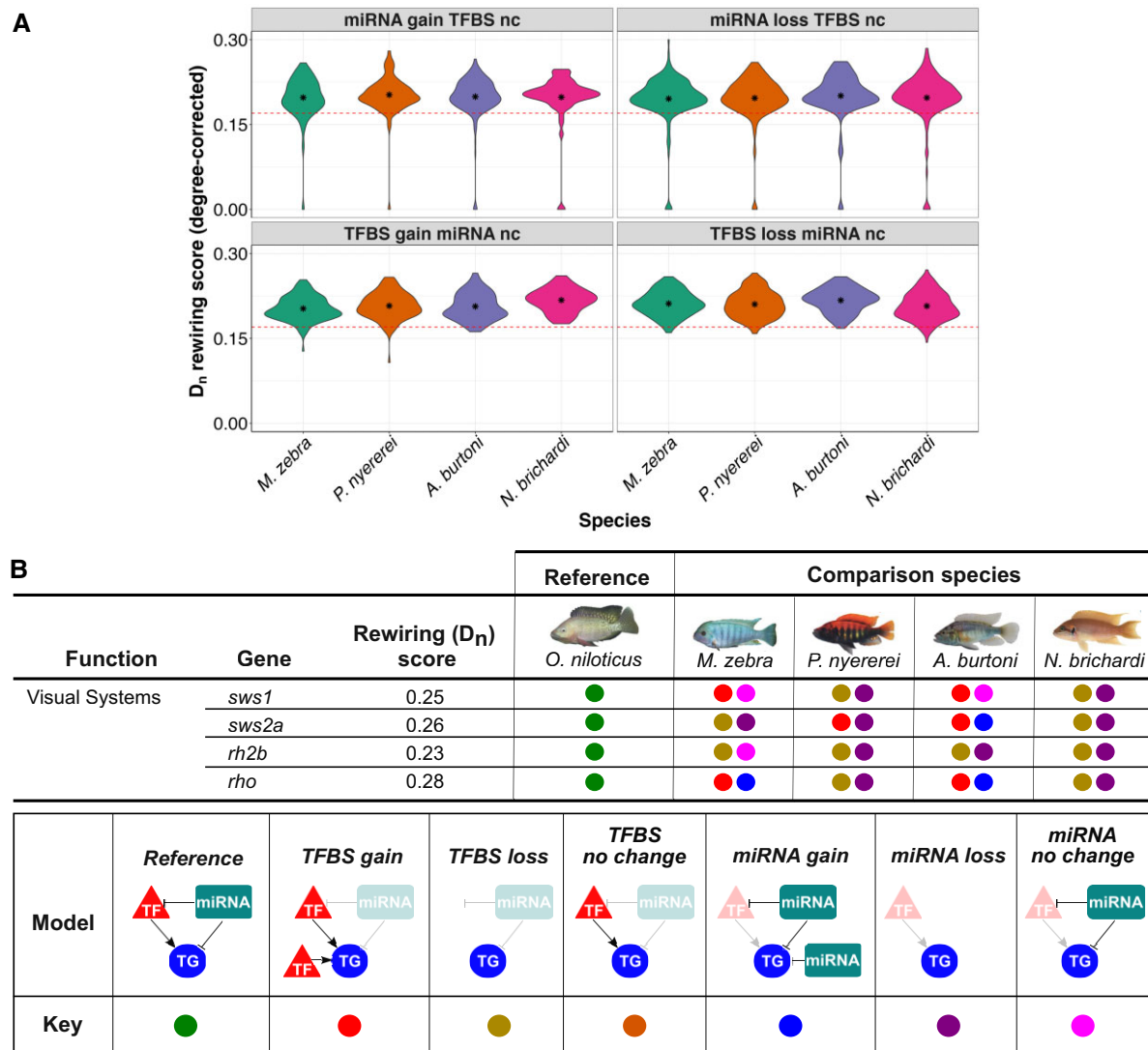


FIG. 4. Binding site evolution in three-node motifs of cichlid genes and their association with rewiring events. (A) Different models of TFBS and miRNA-binding site evolution with associated rewiring rates of 1-to-1 orthogroups in four cichlids. Violin plots of 4/8 models of binding site evolution in each species (x-axis) with DyNet rewiring score of each 1-to-1 orthogroup as degree-corrected D_n score (y-axis). Red-dotted line demarcates a D_n score threshold of 0.17 (for rewired vs. low to nonrewired genes), which was set based on the mean D_n score for all orthogroups in our previous study (Mehta et al. 2021). The term “nc” refers to no change, and mean values are shown as internal asterisk. All statistics are included in [supplementary table S5, Supplementary Material](#) online and violin plots of other models in [supplementary figure S11, Supplementary Material](#) online. (B) Binding site evolution of four cichlid visual system genes. DyNet rewiring (D_n) score for all genes obtained from our previous study (Mehta et al. 2021). For the four comparison species, each gene model of TFBS and miRNA target site evolution in three-node motifs is calculated using the orthologous *O. niloticus* gene as a reference and demarcated as per the “model” and “key” in legend. All statistics are included in [supplementary tables S4 and S5, Supplementary Material](#) online.

divergence in cichlids (Mehta et al. 2021). By investigating binding site evolution in our three-node motifs, we are able to further identify the genetic factors that could be associated with the regulation of opsin expression variation between species. The *sws1* (ultraviolet-sensitive) opsin, utilized as part of the short-wavelength palette in *M. zebra* and *N. brichardi*, has TFBS gain and no change in miRNA-binding site in *M. zebra* and *A. burtoni*, but TFBS and miRNA-binding site loss in the other two species (fig. 4B). In another example, *rhodopsin* (*rho*), associated with dim-light vision in all species, has TFBS and miRNA-binding site gain in *M. zebra* and *A. burtoni*, but TFBS and miRNA-binding site loss in the other

two species (fig. 4B). These patterns of TF and miRNA regulatory divergence, including that of other visual opsins, for example, *sws2a* and *rh2b* (fig. 4B), could therefore contribute to differential expression of adaptive trait genes (see [supplementary information, Supplementary Material](#) online), including visual opsins and their fine-tuning.

Discrete Changes at Regulatory Sites are Fast-Evolving and Associated with Binding Site Turnover

To study the evolution of TF and miRNA regulatory divergence in the five cichlids, we assessed whether regulatory

binding site turnover in three-node motifs is occurring at regions with a different rate of evolution than that expected under a neutral model. We did this by (1) determining the rate of evolution at 4-fold degenerate sites and regulatory regions (3'-UTR, up to 5 kb gene promoter, miRNA-binding sites and TFBSs); (2) identifying between-species variation at regulatory sites and test for accelerated evolution; and (3) assessing corresponding regions in the context of phylogeny and ecology of radiating lake species. We started with 20,106–24,559 (3'-UTR), 19,706–24,123 (up to 5 kb gene promoter), 232,050–478,796 (miRNA-binding sites), and 3,790,407–7,064,048 (TFBSs) unique regulatory regions across the five species, and as a putatively neutrally evolving comparison, 5,292,087–6,539,362 4-fold degenerate sites ([supplementary table S9, Supplementary Material online](#)). The rate of substitutions in whole-genome pairwise comparisons was calculated using phyloP ([Pollard et al. 2010](#)). In total, 86–98% of the nucleotides investigated had mapped conservation–acceleration (CONACC) scores ([supplementary table S9, Supplementary Material online](#)). Across all five species pairwise comparisons, 92% of the 4-fold degenerate sites are conserved, which is consistent with an average of ~6% pairwise divergence at 4-fold sites between *O. niloticus* and the other four species ([Brawand et al. 2014](#)), whereas 3% are evolving at a faster rate than that expected ([supplementary fig. S14 and table S10, Supplementary Material online](#)). On the other hand, 81% of the regulatory regions are conserved, and 4% are exhibiting accelerated evolution ([supplementary fig. S14 and table S10, Supplementary Material online](#)). As our previous study found that discrete regulatory mutations are driving GRN rewiring events ([Mehta et al. 2021](#)), we hypothesized that such mutations could account for some of the accelerated regulatory sites. Using pairwise polymorphic nucleotide sites in each of the four regulatory regions ([supplementary table S12, Supplementary Material online](#)), we identified that 81–87% (3'-UTR), 69–77% (up to 5 kb gene promoter), 83–99% (miRNA-binding sites), and 6–8% (TFBSs) of accelerated sites are accounted for by variation in a single species ([supplementary fig. S15 and table S14, Supplementary Material online](#)). Notably, the proportion of these accelerated sites in the regulatory regions is significantly different (Wilcoxon rank sum test, adjusted *P*-value <0.05, see Materials and Methods), especially between TFBS and miRNA-binding site both within, and between species ([supplementary table S15, Supplementary Material online](#)). These results support the notion that discrete mutations in TFBSs ([Mehta et al. 2021](#)), albeit it very few, and in miRNA-binding sites are fast evolving, that is, fast-evolving regulatory mutations, and drive regulatory binding site turnover in three-node motifs of the five cichlids.

Discrete Changes at Regulatory Sites are Associated with Regulatory Binding Site Turnover in Adaptive Trait Genes

Our previous study identified an abundance of adaptive trait genes with comparatively higher rewired (D_n score >0.17) networks (based on TFBSs), compared with all orthologs ([Mehta et al. 2021](#)). As a measure of regulatory binding site turnover, we therefore sought to test the frequency of association of fast-evolving regulatory mutations in 90 adaptive trait genes ([supplementary table S3, Supplementary Material online](#)) compared with those in corresponding regulatory regions of 90 random “no to low rewired” genes (D_n score ≤0.17) from our previous study ([Mehta et al. 2021](#); see [supplementary information, Supplementary Material online](#)). We used the no to low rewired genes to ensure that the test is not biased toward genes that have rewired GRNs based on TF divergence and using the Wilcoxon rank sum test, tested the frequency 1,000 times to ensure sufficient randomization of no to low rewired (see Materials and Methods). By comparing the proportion of fast-evolving regulatory mutations in corresponding regions of 90 adaptive trait genes and 90 random no to low rewired genes, the most notable differences (>950/1,000 Wilcoxon rank sum tests, adjusted *P*-value <0.05) are found in the proportion of accelerated nucleotides in TFBSs of 90 adaptive trait gene promoter regions ([supplementary table S16, Supplementary Material online](#)). We identified 17 adaptive trait genes with significant turnover between TFBS and miRNA-binding site ([supplementary tables S17 and S18, Supplementary Material online](#)). In *M. zebra*, *P. nyererei*, and *O. niloticus*, this includes genes associated with brain development and neurogenesis, for example, *neurod1*, morphogenesis, for example, *bmpr1*, and visual opsins, for example, *rho* and *sws1* ([supplementary table S17, Supplementary Material online](#)). Furthermore, fast-evolving regulatory mutations of miRNAs and TFs could be associated with the function of adaptive trait genes like, for example, ATF3 associated with neuroprotection of the retina ([Kole et al. 2020](#)) and *miR-99* implicated in retinal regulatory networks ([Andreeva and Cooper 2014](#)) are both predicted to target the visual opsin *sws1*, and *MXI1* associated with neurogenesis ([Klisch et al. 2006](#)) and *miR-212* associated with synaptic plasticity and function ([Remenyi et al. 2013](#)) are predicted to target the dim-light visual opsin, *rho* ([supplementary table S18, Supplementary Material online](#)). Discrete mutations in regulatory binding sites of cichlid adaptive trait genes could therefore be driving GRN evolution associated with traits of cichlid phenotypic diversity.

Discrete Changes at Regulatory Regions of Adaptive Trait Genes Segregate According to Phylogeny and Ecology of Radiating Cichlids

In our previous study, we identified that discrete TFBS mutations driving GRN evolution of visual opsin genes, also segregate according to the phylogeny and ecology of

radiating lake species (Mehta et al. 2021). Here, we extend this approach to study both TFBS and miRNA-binding site variation of three-node motifs in the context of phylogeny and ecology of lake species. Using the Lake Malawi species, *M. zebra*, as a reference, we assess whether regulatory binding site turnover in three-node motifs of this species could be genotypically associated with the ecology of sequenced Lake Malawi species (Malinsky et al. 2018). For this, we started with 827 nucleotide sites that (1) have identified variation between *M. zebra* and any of the other four cichlid species; (2) are located in binding sites of either TFs (709 nucleotide sites) or miRNAs (118 nucleotide sites) of *M. zebra* adaptive trait genes, that also have a significant difference (adjusted *P*-value <0.05) in the proportion of accelerated nucleotides, indicative of regulatory binding site turnover in their associated three-node motifs; and (3) are evolving at a significantly faster rate (adjusted *P*-value <0.05) than expected under a neutral model (supplementary table S18, Supplementary Material online). We identified that 94 out of 827 accelerated nucleotide sites with between-species variation across 73 Lake Malawi species also exhibit flanking sequence conservation, representative of shared ancestral variation. Of the 94 accelerated nucleotide sites, 21 are found in miRNA-binding sites, and 73 are found in TFBSs of which, 55 were not identified in our previous study (Mehta et al. 2021) due to not incorporating substitution rates. Among the 76 accelerated nucleotide sites uniquely identified in this study, 15 (20%) include TFBS and miRNA-binding site variation of visual opsin genes. Given the variability and importance of visual systems toward cichlid foraging habits, we therefore focus on variation at accelerated regulatory regions of visual opsin genes. If the TFBS and miRNA-binding site are likely functional, we hypothesize that radiating species with similar foraging habits would share conserved regulatory genotypes, to possibly regulate and tune similar spectral sensitivities; whereas distally related species with dissimilar foraging habits would segregate at the corresponding regulatory site.

We first focus on a three-node motif of the *M. zebra* short-wavelength palette visual opsin gene, *sws1*, that is predicted to be regulated by *miR-99a* and ATF3 (fig. 5A).

The homozygous variant (C|C) that predicts binding of *miR-99a* to *M. zebra sws1* 3'-UTR (fig. 5A) is (1) conserved in 60/134 (45%) Lake Malawi individuals, including the fellow algae eater, *Tropheops tropheops*, and other distantly related species, for example, *Dimidiochromis kiwinge* and *Nimbochromis polystigma*, that utilize the same short-wavelength palette; but (2) lost in the other four species due to the A/A homozygous variant (fig. 5A) and also homozygous segregated (A|A) in 38/134 (28%) Lake Malawi individuals, including its most closely related Mbuna species (*Petrotilapia genalutea*) and *A. calliptera* (fig. 5B and supplementary fig. S17, Supplementary Material online). Another homozygous variant (C|C), that predicts binding of ATF3 to *M. zebra sws1* gene promoter, but is lost in *O. niloticus*, due to the T/T homozygous variant (fig. 5A), is (1) conserved in all closely

related Mbuna species and 102/116 (88%) Lake Malawi individuals, including the closely related *A. calliptera* clade; but (2) heterozygous or homozygous segregating in distantly related Lake Malawi species that utilize the same short-wavelength palette, but occupy different habitats and foraging habits, for example, *D. kiwinge*—T|T and *N. polystigma*—T|C (fig. 5B and supplementary fig. S16, Supplementary Material online). Overall, this suggests that although *miR-99a* could be core regulator of *sws1* in nearly half of the studied Lake Malawi species, it is (1) unlikely to be a co-regulator of *sws1* (with ATF3) in either distantly related Lake Malawi species utilizing the short-wavelength palette, for example, *D. kiwinge* and *N. polystigma*, or the *A. calliptera* clade; but (2) likely to co-regulate *sws1* (with ATF3) in most members of the rock-dwelling Mbuna clade (fig. 5B, supplementary figs. S16 and S17, Supplementary Material online). In another example, we show that a three-node motif of the dim-light vision gene, *rho*, consisting of *miR-212* and MXI1 has conserved regulatory genotypes in all studied Lake Malawi species, but has segregated and therefore not predicted in the other four cichlids (supplementary figs. S18 and S19, Supplementary Material online). Phylogenetic independent contrast (PIC) analysis (Felsenstein 1985) of the *sws1* (supplementary figs. S20 and S21, Supplementary Material online) and *rho* (supplementary figs. S22 and S23, Supplementary Material online) genotypes against visual traits and ecology of each of the 73 Lake Malawi species, highlights very little change in correlation once the phylogeny is taken into account and a regression model fitted (see Materials and Methods). In summary, we identified three-node motifs of visual systems that segregate according to phylogeny and ecology of lake species. Regulatory binding site turnover of three-node motifs is therefore a key contributing mechanism of GRN evolution associated with adaptive innovations in East African cichlid radiations.

Discussion

Evolutionary changes of regulatory systems and GRN rewiring events can contribute to the evolution of phenotypic diversity and rapid adaptation (Kratochwil and Meyer 2015). This is particularly the case for East African cichlid diversification that has been shaped by complex evolutionary and genomic forces. These include divergent selection acting upon regulatory regions that can alter gene expression programs (Brawand et al. 2014), rapid evolution of noncoding RNA expression (El Taher et al. 2021), and ancient polymorphisms in noncoding regions (McGee et al. 2020), contrasted against a background of low between-species genetic diversity (Malinsky et al. 2018; McGee et al. 2020; Ronco et al. 2021). All of these findings imply that discrete differences at regulatory regions could contribute to phenotypic differences and indeed, through discrete changes in TFBSs, we previously showed that GRN rewiring could be a key contributor to cichlid phenotypic diversity (Mehta et al. 2021). However, our previous study did not explore

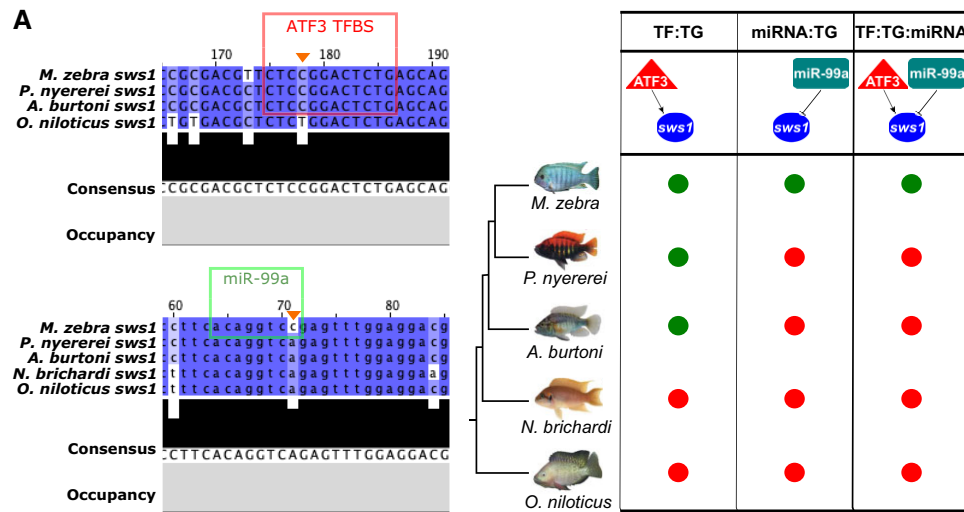
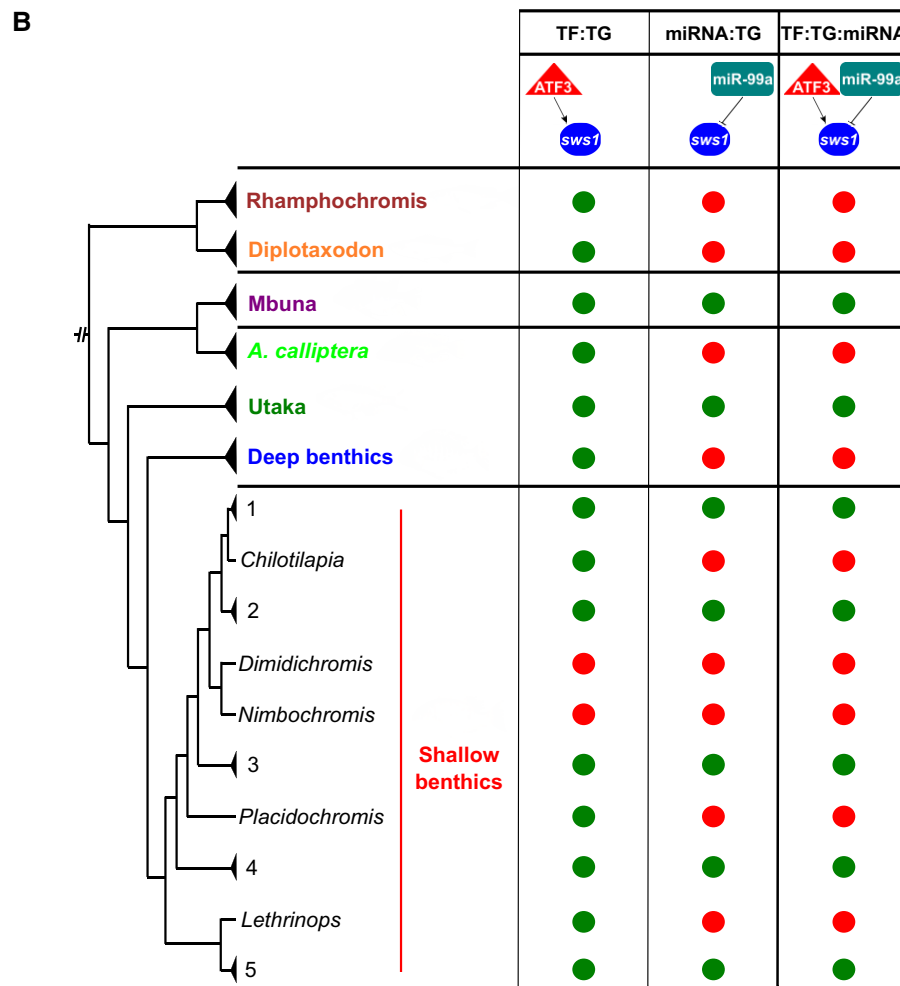


FIG. 5. Evolution of the ATF3:sws1:miR-99a three-node motif in the five cichlids and Lake Malawi species. (A) On the top left, ATF3 motif prediction in *M. zebra*, *P. nyererei*, and *A. burtoni* sws1 gene promoter (red box) and substitution demarcated in *O. niloticus* sws1 gene promoter (orange arrow). On the bottom left, miR-99a-binding site prediction in *M. zebra* sws1 3'-UTR (green box) and substitution demarcated in *P. nyererei*, *A. burtoni*, *N. brichardi*, and *O. niloticus* sws1 3'-UTR (orange arrow). According to these predicted sites, evolution of the ATF3:sws1:miR-99a three-node motif in the five cichlid phylogeny is depicted based on presence (green circle) and absence (red circle). (B) Simplified presence (green circle) and absence (red circle) of the ATF3:sws1:miR-99a three-node motif in Lake Malawi species based on SNP genotypes overlapping ATF3 TFBS and miR-99a-binding sites in *M. zebra* sws1 gene promoter and 3'-UTR (orange arrows, A). Lake Malawi phylogeny reproduced from published ASTRAL phylogeny (Malinsky et al. 2018). Phylogenetic branches labelled with genus, species, or clade identifiers. Within the shallow benthics, species within some clades are summarized by numbers: 1 = *Hemitaeniochromis*, *Protomelas*; 2 = *Hemilitapia*, *Otopharynx*, *Mylochromis*; 3 = *Champsocromis*, *Tyrannochromis*, *Trematocranus*, *Otopharynx*, *Mylochromis*, *Stigmatochromis*, *Taeniochromis*, *Buccochromis*, *Ctenopharynx*; 4 = *Mylochromis*; 5 = *Taeniolethrinos*. Expanded genotype, phenotype, and ecotype phylogeny in supplementary figures S16 and S17, Supplementary Material online.



and integrate other genetic mechanisms, like the contributions of miRNAs toward cichlid GRN evolution. Given that miRNAs are key regulators of posttranscriptional gene expression, and that novel miRNAs have evolved in rapidly radiating cichlids (Brawand et al. 2014; Franchini et al. 2016, 2019; Xiong et al. 2019), they could therefore contribute to GRN evolution associated with cichlid phenotypic diversity.

Across the five cichlid species, we identified a total of 15,390,993 binding sites for the 18,799 co-expressed orthogroups. The total number of sites is inflated compared with the 38,768 putative miRNA-binding sites predicted in the Midas genome (Franchini et al. 2016) due to (1) a difference of approaches whereby, Franchini et al. use miRanda (John et al. 2004) for target prediction,

a tool that is found to predict fewer experimentally derived sites as compared with Targetscan7 (Agarwal et al. 2015; Riffo-Campos et al. 2016); (2) retention of multiple sites for the same miRNA along a 3'-UTR to analyze nucleotide variation at all predicted sites, like that previously applied for all TFBSs in corresponding gene promoter regions (Mehta et al. 2021); and (3) we predict binding sites in an average of 13,998 3'-UTRs, which is 41% more (8,232 3'-UTRs) than in the Midas genome (Franchini et al. 2016). Despite these differences, we identify an average of 356,379 unique miRNA-binding sites across the five species, ranging from 1 to 173 unique miRNA-binding sites per 3'-UTR, that is comparable with the range (0–222) previously identified in Midas cichlids (Franchini et al. 2016). Across the five species, 3'-UTR-binding sites are differentially predicted for up to 172 miRNA families. The underrepresentation of certain families in a species can be attributed to mutations of the seed sequence and *arm* switching (Berezikov 2011; Brawand et al. 2014). The largest number of conserved miRNA families are across all five species and include binding sites in 3'-UTRs of genes associated with jaw development (Bloomquist et al. 2017) and deep-water adaptation (Hahn et al. 2017). This supports an important regulatory role of miRNAs to cichlid adaptive traits (Brawand et al. 2014) over a divergence time of ~19 My (Hughes et al. 2018). We identified more miRNA family divergence within the haplochromine lineage, particularly in 3'-UTRs of developmental genes; a finding that is consistent with rapid evolutionary changes of noncoding RNA expression (El Taher et al. 2021) and noncoding regions (McGee et al. 2020) in corresponding Lake Tanganyika and Victoria species. Our results suggest a deeply conserved role of miRNA regulation in the five cichlids; however, binding site divergence of miRNA families is likely to have an important gene regulatory role in the rapid (~6 My; Hughes et al. 2018) phenotypic divergence of haplochromines.

As a GRN can be composed of both transcriptional activation and repression, we extended our previous study (Mehta et al. 2021) to focus on a miRNA-FFL three-node motif. Using this three-node motif as a measure of network divergence and evolutionary constraint, we identified increased novel/species-specific three-node motifs overall, reflected by a higher rate of miRNA edge loss (than TF edge loss) along the phylogeny. This is consistent with previous findings in Midas cichlids where miRNAs and concomitantly, their binding sites, can be rapidly lost between related groups (Xiong et al. 2019). In support, we tested the association of eight models of TFBS and/or miRNA-binding site evolution, including no change, on TG edges previously defined as low to nonrewired (Mehta et al. 2021) based on TFBSs only. We found that the most associations were expectedly with no change in TFBS, and miRNA-binding site loss in all four species compared with *O. niloticus* as a reference. This indicates that miRNA-binding site loss is having a discrete impact on GRN rewiring but overall, different models of regulatory binding site evolution have impacted GRN rewiring in

the cichlid lineages studied here. This included identifying that the most associated model of four highly rewired visual opsin genes (*sws1*, *rho*, *sws2a*, and *rh2b*; Mehta et al. 2021) was generally TFBS (in 50%) and miRNA-binding site (in 66%) loss across the species. This supports our previous work demonstrating that opsin expression diversity could be the result of TFBS divergence in cichlids (Mehta et al. 2021) and thus, regulatory divergence is likely to accommodate for heterochronic shifts in opsin expression (Carleton et al. 2008; O'Quin et al. 2011). Overall, these findings suggest that differential patterns of TF and miRNA regulatory divergence are likely to be associated with three-node motif and GRN rewiring of cichlid adaptive traits.

Across all five species pairwise comparisons, we find that regulatory divergence, that is, binding site turnover in three-node motifs is occurring at regions with a different rate of evolution than that expected under a neutral model. This is supported by a previous study that also identified evolutionary-accelerated 3'-UTRs in the same five cichlid species and overall, suggested this as a contributory mechanism for speciation (Puntambekar et al. 2020). However, we extend all previous work to show that on average, nearly a third of all fast-evolving nucleotide sites in the four regulatory regions (3'-UTR, up to 5 kb gene promoter, miRNA-binding sites and TFBSs) can be explained by pairwise polymorphisms in a single species. Although more than 83% of fast-evolving nucleotides in miRNA-binding sites are accounted for variation in a single species, <8% of TFBSs are accounted for by the same type of fast-evolving variation. This supports our previous finding of discrete mutations in TFBSs driving GRN rewiring events (Mehta et al. 2021), as well as elevated single-nucleotide polymorphism (SNP) densities in predicted miRNA-binding sites, compared with flanking 3'-UTR regions, of five Lake Malawi species (Loh et al. 2011). Positive selection acting upon these regulatory regions is therefore likely to be an important evolutionary force in rapidly radiating cichlids. This is especially the case for adaptive trait genes such as the visual opsins, for example, *rho* and *sws1*, that we show to exhibit a higher proportion of fast-evolving nucleotides in their TFBS and miRNA-binding site, compared with subsets of random genes. Furthermore, these TFs and miRNAs are generally functionally associated with their TG in predicted three-node motifs like, for example, the visual opsin gene, *sws1*, is predicted to be co-regulated by the TF, ATF3, that is associated with neuroprotection of the retina (Kole et al. 2020) and *miR-99* implicated in retinal regulatory networks (Andreeva and Cooper 2014). The regulatory variants of this three-node motif (ATF3 > *sws1* < *miR-99a*) in *M. zebra* also appear to differentially segregate according to phylogeny and ecology of Lake Malawi species (Malinsky et al. 2018). We find that ATF3:*miR-99a* could be an important regulator of *sws1* in the rock-dwelling Mbuna clade, but unlikely to co-regulate *sws1* as part of the short-wavelength palette in the *A. calliptera* clade and distantly related Lake Malawi species. For another opsin gene, we identified that the possible neural co-regulation of *rho*, and therefore dim-

light vision response by MX11:miR-212, could be a Lake Malawi specific regulatory innovation. Overall, differential binding of miRNAs and TFs associated with retinal sensory modalities (Loh et al. 2011) and visual tuning (Sandkam et al. 2020) is likely to be an important genetic mechanism contributing to Lake Malawi species visual adaptations. Although these results significantly expand our previously characterized visual opsin GRNs (Mehta et al. 2021) and provide insights into their evolution in radiating cichlids, we also provide support for the hypothesis that the evolution of cichlid visual tuning has been facilitated by regulatory mutations that are constrained by mutational dynamics (Nandamuri et al. 2018; Sandkam et al. 2020). Differential regulation of opsin genes in three-node motifs between cichlid species and their implications toward visual tuning could correspond to diversity of foraging habits, diet, habitat choice, and also nuptial coloration. Fitting the Lake Malawi phylogeny had little effect on the correlations between regulatory genotypes, and visual/ecologic characteristics, and therefore suggests covariance between TF/miRNA regulatory genotypes and traits. However, similar to our previous study (Mehta et al. 2021), weak correlation suggests that ecotype-associated three-node motif and GRN rewiring require additional testing. This analysis would further benefit from (1) supplementing any missing data (of wavelength palette, habitat and/or foraging habit/diet); (2) adding species data from any lowly represented clades, for example, Mbuna; and (3) experimental testing of the predicted sites.

Alongside our previous study (Mehta et al. 2021), the three-node motifs and extended GRNs generated here represent a unique resource for the community; powering further molecular and evolutionary analysis of cichlid adaptive traits. For example, further examination of the three-node motifs predicted for the visual systems, that could co-regulate opsin expression diversity, could further shed light on previous preliminary studies (Carleton et al. 2008; Hofmann et al. 2009; O'Quin et al. 2012; Nandamuri et al. 2018; Sandkam et al. 2020). This could involve functional validations of three-node motifs to observed trait variation by (1) high-throughput miRNA-mRNA complex and protein-DNA assays to confirm binding of thousands of sites; (2) reporter and/or cell-based assays to demonstrate transcriptional regulation; and (3) genome editing, for example, CRISPR mutations of regulatory variants to test for any observed phenotypic effect. Nonetheless, by studying the impact of miRNA regulation in three-node motifs, this work extends the first genome-wide exploration of GRN evolution in cichlids (Mehta et al. 2021). In a wider context, as the individual regulatory hallmarks of TFs and miRNAs start to become characterized in disease, for example, forms of cancer (Plaisier et al. 2016; Mullany et al. 2018; Nersisyan et al. 2021), congenital heart disease (You et al. 2020), neuromuscular disorders (Bo et al. 2021), as well as related to gene expression in human tissues (Minchington et al. 2020) and plant stress response (Sharma et al. 2020, 2021), the computational framework we applied here could be used to study the evolution of characterized regulatory edges and GRNs in the aforementioned, and other systems and phylogenies. However, the combined

framework could be extended further by (1) analyzing the impact of either more, or all of the 104 three-node motif models (Ahnert and Fink 2016) through the integration of epigenetic and co-immunoprecipitation assay data to gain regulatory directionality; and (2) including relevant data sets to study the regulatory effect of other mechanisms, for example, lncRNAs and enhancers on network topology, that could also contribute toward the evolution of cichlid phenotypic diversity (Brawand et al. 2014; Salzburger 2018). Although many of the predicted three-node motifs could be false positives, the approach applied here and previously (Mehta et al. 2021) ensured for rigorous filtering at each step; this included stringent statistical significance measures, and all although accounting for any node loss and mis-annotations in selected species (see Materials and Methods).

In summary, cichlids appear to utilize an array of genetic mechanisms that also contribute toward phenotypic diversity in other organisms (Wittkopp et al. 2008; Yanai and Hunter 2009; Chan et al. 2010; Jones et al. 2012; Thompson et al. 2013; Ichihashi et al. 2014). However, here we provide support of TF and miRNA co-regulatory rewiring in three-node motifs of genes associated with adaptive traits in cichlids. This is further supported by large-scale genotyping studies of the predicted regulatory sites in rapidly radiating cichlid species (Malinsky et al. 2018). This potential link between the evolution of three-node motifs as part of GRNs associated with cichlid adaptive traits requires further experimental verification. This is beyond that described for *cis*-regulatory sites previously (Mehta et al. 2021), as well as support based on large-scale genotyping (Malinsky et al. 2018; McGee et al. 2020; Ronco et al. 2021) and transcriptome evolution (El Taher et al. 2021); epigenetic divergence (Kratochwil and Meyer 2014; Vernaz et al. 2021); transgenesis assays (Brawand et al. 2014; Santos et al. 2014); population studies and CRISPR mutant assays (Kratochwil et al. 2018); and transcriptomic/*cis*-regulatory assays (Hofmann et al. 2009; O'Quin et al. 2010; Nandamuri et al. 2018; Sandkam et al. 2020) of cichlid species.

Materials and Methods

Genomic and Transcriptomic Resources

Genomes and transcriptomes of the five cichlid species were obtained from NCBI and corresponding publication (Brawand et al. 2014): *P. nyererei*—PunNye1.0, NCBI BioProject: PRJNA60367; BROADPN2 annotation; *M. zebra*—MetZeb1.1, NCBI BioProject: PRJNA60369; BROADMZ2 annotation; *A. burtoni*—AstBur1.0, NCBI BioProject: PRJNA60363; BROADAB2 annotation; *N. brichardi*—NeoBri1.0, NCBI BioProject: PRJNA60365; BROADNB2 annotation; and *O. niloticus*—Orenil1.1 (NCBI BioProject: PRJNA59571; BROADON2 annotation).

MicroRNA Target Prediction

We used the miRNAs that were previously sequenced from whole embryo for five cichlid species (*O. niloticus*, *N. brichardi*,

A. burtoni, *P. nyererei*, and *M. zebra*; Brawand et al. 2014). The miRNA mature sequences and hairpin structures have been characterized as described previously (Brawand et al. 2014) and deposited in miRbase (Kozomara and Griffiths-Jones 2014). A total of 992 (On-198, Nb-183, Ab-243, Mz-185, Pn-183) cichlid miRNA mature sequences and annotated 3'-UTRs of 21,871 orthogroups (On-22411, Nb-20195, Ab-22662, Mz-21918, and Pn-21599) in all five species (Brawand et al. 2014) were used for target prediction. We used TargetScan7 (Agarwal et al. 2015) to predict species-specific genes targeted by the sequenced miRNAs. We used *mafft-7.271* (Katoh and Standley 2013) to generate gene-specific multiple alignments of the annotated 3'-UTRs across all five cichlid species. Target predictions were obtained by running TargetScan7 (v7.2; Agarwal et al. 2015) according to the developer's protocols with default parameters. Firstly, miRNA-binding sites were predicted using the reformatted alignments and the sequenced mature miRNA sequences as input for the "targetscan_70.pl" script with default parameters. Using the median branch length (BL) from each 3'-UTR alignment derived from the "targetscan_70_BL_bins.pl" script and predicted miRNA-binding sites, we then calculated the conserved BL and probability of preferentially conserved targeting (PCT) for all predicted miRNA targets using the "targetscan_70_BL_PCT.pl" script with default PCT and parameters as derived from https://www.targetscan.org/vert_72/vert_72_data_download/targetscan_70_BL_PCT.zip and (Agarwal et al. 2015). All seed sites were found and counted in 3'-UTR sequences using the "targetscan_count_8mers.pl" script. Finally, to predict high-confidence miRNA targets that could be as predictive as the most informative in vivo approaches such as crosslinking-immunoprecipitation (CLIP; Agarwal et al. 2015), we used the miRNA mature sequences, 3'-UTR alignments, calculated BL and PCT scores and seed site locations with counts as input to the "targetscan_70_context_scores_cichlids.pl" script to calculate Targetscan7 weighted context++ scores. The developers of Targetscan7 found that the context++ model was more predictive than any published model for miRNA targeting efficacy, and as predictive as the most informative in vivo crosslinking approaches, for example, CLIP (Agarwal et al. 2015). The weighted context++ score ranges from 1 to -1 and thus, scores with a lower negative value indicate a greater prediction of repression (Agarwal et al. 2015). Based on previous predictions of miRNA targets using Targetscan7 in vertebrates (Warnefors et al. 2017; Hu et al. 2019; Sayed and Park 2020), we selected all targets using a stringent weighted context++ score lower than -0.1 to filter out low quality predictions; these were the binding sites used for analyses.

The multiple alignments of annotated 3'-UTRs and positions of predicted sites in each species were used to identify overlapping miRNA-binding sites of miRNA families between species.

GO Enrichment

To assess enrichment of GO terms in a given gene set, we use the Benjamini-Hochberg (BH; Benjamini and

Hochberg 1995) FDR corrected hypergeometric *P*-value (*q*-value). The background (control set) for the enrichment analysis is composed of all co-expressed genes (18,799 orthogroups) from our previous study (Mehta et al. 2021). GO terms for the five cichlids were extracted from those published previously (Brawand et al. 2014).

TF Motif Scanning

To study TF-TG associations in three-node motifs, we used predicted TFBSs from our previous study (Mehta et al. 2021). Briefly, we used the aforementioned published assemblies and associated gene annotations (Brawand et al. 2014) for each species to extract gene promoter regions, defined as up to 5 kb upstream of the transcription start site of each gene. We used a combination of (1) JASPAR vertebrate motifs; (2) extrapolated cichlid species-specific (CS) position-specific scoring matrices (PSSMs; Mehta et al. 2021); and (3) aggregated generic cichlid-wide PSSMs (Mehta et al. 2021) to identify TF motifs. Using Find Individual Motif Occurrences (FIMO) (Grant et al. 2011), the gene promoter regions of each species were scanned for each TF motif using either (1) an optimal calculated *P*-value for each TF PSSM, as calculated using the *matrix quality* script from the RSAT tool suite (Medina-Rivera et al. 2015); or (2) FIMO (Grant et al. 2011) default *P*-value ($1e-4$) for JASPAR (Khan et al. 2018) PSSMs and PSSMs for which an optimal *P*-value could not be determined. Statistically significant TFBS motifs (FDR < 0.05) were associated with their proximal TG and represented as two nodes and one TF-TG edge. In total, there were 3,295,212–5,900,174 predicted TF-TG edges (FDR < 0.05) across the five species (Mehta et al. 2021). This was encoded into a matrix of 1,131,812 predicted TF-TG edges (FDR < 0.05), where each edge is present in at least two species (Mehta et al. 2021). To enable accurate analysis of GRN rewiring and retain relevant TF-TG interactions, all collated edges were pruned to a total of 843,168 TF-TG edges (FDR < 0.05) where (1) the edge is present in at least two species; (2) edges are not absent in any species due to node loss or mis-annotation; and (3) based on the presence of nodes in modules of co-expressed genes in our previous study (Mehta et al. 2021).

Three-Node Motif Generation

Three-node motifs in our study are defined as a miRNA-FFL, where a TF is predicted to regulate a TG and a miRNA is predicted to directly regulate either the TF or TG (fig. 3A). Three-node motifs (TF:TG:miRNA) were encoded by merging all combinations of predicted TF and miRNA interactions of a TG.

Three-Node Motif Analysis

For each species three-node motifs, all TF:miRNA nodes were extrapolated for all TGs and their frequency recorded (based on the same TF orthogroup and miRNA family classification). By reverse ranking the frequency of all TF:miRNA nodes in each species, the top 100 relationships

were classified to test for any significant overlap of TFs and miRNAs in species-specific three-node motifs.

A presence–absence matrix of three-node motifs in each species was generated, and the number of TFBS and miRNA-binding site gains and losses, against predictions in *O. niloticus*, were calculated for each species TG. The degree-corrected rewiring (D_n) score of TF–TG interactions in each orthogroup, as inferred by the DyNet-2.0 package (Goenawan et al. 2016) implemented in Cytoscape-3.7.1 (Franz et al. 2015), was then mapped for GRN rewiring analysis.

Hypergeometric Tests for Regulatory Site Gain and Loss Enrichment

The *phyper* function in R (v4.0.2) was used to test for enrichment of rewired (degree-corrected D_n score >0.17) or low to nonrewired (degree-corrected D_n score ≤ 0.17) genes in each of the eight models of TFBS and/or miRNA-binding site gains, losses, or no change. The D_n score threshold of 0.17 (for rewired vs. low to nonrewired) was set based on the mean D_n score for all orthogroups and as a measure of significantly rewired genes based on our previous study (Mehta et al. 2021). A threshold of P -value <0.05 was used as a measure of significant enrichment.

Calculating Substitution Rate at Regulatory Regions

To identify loci evolving at a faster rate than that expected under a neutral model, we used phyloP (Pollard et al. 2010) from the Phylogenetic Analysis with Space/Time Models (PHAST) v1.5 package (Hubisz et al. 2011). This was carried out on the previously published five-way *multiz* multiple alignment file (MAF) centered on *O. niloticus* v1.1 (Brawand et al. 2014). An *O. niloticus* centered MAF was used as a reference owing to its phylogenetic position as an outgroup to study substitution rates within the cichlid phylogeny and radiating lake species. Using the *O. niloticus* centered MAF, a neutral substitution model was constructed using the previously published five cichlid phylogeny (Brawand et al. 2014) in phyloFit from PHAST v1.5 (Hubisz et al. 2011) by fitting a time reversible substitution “REV” model. The multiple alignment was split by chromosome/scaffold and phyloP (Pollard et al. 2010) ran using the likelihood ratio test (LRT) and the “all branches” test to predict CONACC scores for each site in the five species multiple alignment.

To obtain pairwise phyloP scores, we (1) created MAFs that are centric to each of the other four species by reordering the original *O. niloticus* centered MAF using mafOrder from UCSC kent tools v333. Regardless of the species, the same alignment information is therefore retained throughout the workflow; (2) removed all alignments that excluded the reference species using mafFilter from UCSC kent tools v333; (3) created sorted MAFs for all pairwise species combinations using the mafFilter function in mafTools v0.1 (Earl et al. 2014); (4) constructed a neutral substitution model for each pairwise combination using phyloFit from PHAST v1.5 (Hubisz et al.

2011) by fitting a time reversible substitution “REV” model; (5) split each pairwise MAF by chromosome/scaffold; and (6) calculated substitution rates in phyloP (Pollard et al. 2010) using the LRT and the “all branches” test to predict CONACC using each corresponding pairwise neutral substitution model. To compare CONACC scores of regulatory regions to neutrally evolving regions, 4-fold degenerate sites were extracted from each genome using an in-house perl script that takes a gene annotation as gene transfer format file, whole-genome FASTA file and 4-fold degenerate codon table as input. The phyloP scores were then mapped to 4-fold degenerate sites and the four regulatory regions (3'-UTR excluding miRNA-binding sites, up to 5 kb gene promoter excluding TFBSs, 3'-UTR miRNA-binding sites and up to 5 kb gene promoter TFBSs) of each species using bedtools-2.25.0 intersect (Quinlan and Hall 2010).

Identification of Pairwise Variation between the Five Species

After stage three of the above where pairwise species MAFs are created by sorting and filtering each species centric MAF, there were a total of 20 MAFs representing all pairwise species combinations (5 ref species \times 4 comparison species). Each pairwise species MAF was used to identify pairwise variation using a custom python script “get_subs_from_maf.py.” Pairwise (single-nucleotide) variants were mapped to the phyloP scores of four regulatory regions (3'-UTR, up to 5 kb gene promoter, miRNA-binding sites, and TFBSs) using bedtools-2.25.0 intersect (Quinlan and Hall 2010).

Testing the Significance of Difference in CONACC Scores of Pairwise Variation in Regulatory Regions

The significance of CONACC scores of pairwise polymorphic nucleotide sites in regulatory regions of all species was tested both within and between species using the Wilcoxon rank sum test. The P -values were adjusted for multiple test correction using the BH method (Benjamini and Hochberg 1995). The adjusted P -value was recorded as either having a significant (adjusted P -value <0.05) or insignificant (adjusted P -value >0.05) difference in CONACC scores of pairwise polymorphic nucleotide sites in within and between regulatory regions of all five species.

Testing the Significance of CONACC Scores in Regulatory Regions of Adaptive Trait Genes

The significance of CONACC scores of pairwise polymorphic nucleotide sites in regulatory regions of 90 adaptive trait genes was tested by: (1) randomly picking up to 90 no to low rewired genes (D_n score ≤ 0.17) from our previous study (Mehta et al. 2021), 1000 times; and (2) testing (Wilcoxon rank sum) the difference in CONACC scores of pairwise polymorphic nucleotide sites in each regulatory region of the 90 random genes to the corresponding regulatory region of all 90 adaptive trait genes. The P -values were adjusted for multiple test correction using the BH method (Benjamini and Hochberg 1995). The number of

times (from 1,000 tests) was recorded as either having a significant (Wilcoxon rank sum test, adjusted P -value <0.05) or insignificant (Wilcoxon rank sum test, adjusted P -value >0.05) difference in CONACC scores of pairwise polymorphic nucleotide sites in each regulatory region of all five species. The adjusted P -values derived from Wilcoxon rank sum tests, between CONACC scores of polymorphic nucleotide sites in the regulatory region of 90 adaptive trait genes were ranked, and reverse sorted, to identify significant (adjusted P -value <0.05) regulatory binding site turnover.

Identification of Segregating Variants within Binding Sites

Pairwise variants of *M. zebra* were overlapped with SNPs in Lake Malawi species (Malinsky et al. 2018) using *bedtools*-2.25.0 intersect (Quinlan and Hall 2010). The pairwise variants overlapping binding sites and lake species SNPs were then filtered based on the presence of the same pairwise variant in orthologous 3'-UTR alignments. This ensured concordance of whole-genome alignment-derived variants with variation in 3'-UTR alignments and predicted binding sites. At each step, complementation of reference and alternative alleles was accounted for to ensure correct overlap. This analysis was not carried out to distinguish population differentiation due to genetic structure, but to instead map 3'-UTR regulatory variants onto a number of radiating cichlid species to link to phylogenetic and ecologic traits.

Phylogenetic Independent Contrasts

PICs were carried out to statistically test the effect of fitting the 73 Lake Malawi species phylogeny (Malinsky et al. 2018) to the covariance of segregating TFBSs and miRNA-binding site, visual (wavelength palette) and ecologic traits (habitat and foraging habit/diet). This involved (1) categorically coding the genotypes of segregating regulatory sites, visual trait, and ecologic measurements for each of the 73 Lake Malawi species (119 individuals), and (2) using the *ape* package (v5.4.1) in R (v4.0.2) to apply the PICs test (Felsenstein 1985) on all correlations with the binding site genotype (genotype vs. wavelength palette, genotype vs. habitat, and genotype vs. foraging habit/diet). PICs assume a linear relationship and a process of Brownian motion between traits, and thus, for each combination of data, scatterplots were first generated. To test for any change in the correlation owing to phylogenetic signal, the regression model was compared between the relationships both excluding and including the Lake Malawi phylogeny (Malinsky et al. 2018).

Supplementary Material

Supplementary data are available at *Molecular Biology and Evolution* online.

Acknowledgment

The authors thank the BROAD institute and the Cichlid Genome Consortium for providing full access to genomic data. This work was supported by the Biotechnological and Biosciences Research Council (BBSRC), part of UK Research and Innovation, Institute Strategic Programme (grant number BB/J004669/), Core Strategic Programme Grants (grant numbers BB/P016774/1, BBS/E/T/000PR9817, BB/CSP17270/1, and BB/CCG1720/1) to T.K.M., L.P.D., W.N., F.D.P., and W.H. at the Earlham Institute, and acknowledges the work delivered via the Scientific Computing group, as well as support for the physical HPC infrastructure and data center delivered via the NBI Computing infrastructure for Science (CiS) group. This work was also supported by a National Science Foundation (NSF) career award (grant number 1350677 to S.R.) and the McDonnell foundation at The Wisconsin Institute for Discovery.

Author Contributions

T.K.M. ran GO enrichment, three-node motif generation, analyzed three-node motifs, tested regulatory site gain and loss, calculated substitution rates, identified pairwise variants, tested the significance of CONACC scores, identified segregating binding sites, and ran PIC tests; L.P.D. ran miRNA target prediction; W.N. ran TF motif scanning; T.K.M. and W.H. wrote the manuscript with input from L.P.D., W.N., S.R., and F.D.P.

Conflict of interest: The authors declare that they have no competing interests.

Data Availability

Data underlying this article are available in the article and in its online [supplementary material](#).

References

- Agarwal V, Bell GW, Nam J-W, Bartel DP, Ameres SL, Martinez J, Schroeder R, Anders G, Mackowiak SD, Jens M. 2015. Predicting effective microRNA target sites in mammalian mRNAs. *eLife* 4:101–112. doi:10.7554/eLife.05005
- Ahnert SE, Fink TMA. 2016. Form and function in gene regulatory networks: the structure of network motifs determines fundamental properties of their dynamical state space. *J R Soc Interface* 13:20160179–20160179. doi:10.1098/rsif.2016.0179
- Albertson RC, Kawasaki KC, Tetrault ER, Powder KE. 2018. Genetic analyses in Lake Malawi cichlids identify new roles for Fgf signaling in scale shape variation. *Commun Biol*. 1:55. doi:10.1038/s42003-018-0060-4
- Alon U. 2007. Network motifs: theory and experimental approaches. *Nat Rev Genet*. 8:450–461. doi:10.1038/nrg2102
- Andreeva K, Cooper NGF. 2014. MicroRNAs in the neural retina. *Int J Genomics* 2014:165897–165897. doi:10.1155/2014/165897
- Benjamini Y, Hochberg Y. 1995. Controlling the false discovery rate: a practical and powerful approach to multiple testing. *J R Stat Soc B* 57(1):289–300.
- Berezikov E. 2011. Evolution of microRNA diversity and regulation in animals. *Nat Rev Genet*. 12(12):846–860. doi:10.1038/nrg3079

- Bloomquist RF, Fowler TE, Sylvester JB, Miro RJ, Streelman JT. 2017. A compendium of developmental gene expression in Lake Malawi cichlid fishes. *BMC Dev Biol.* **17**(1):3–3. doi:10.1186/s12861-017-0146-0
- Bo C, Zhang H, Cao Y, Lu X, Zhang C, Li S, Kong X, Zhang X, Bai M, Tian K, et al. 2021. Construction of a TF–miRNA–gene feed-forward loop network predicts biomarkers and potential drugs for myasthenia gravis. *Sci Rep.* **11**(1):2416–2416. doi:10.1038/s41598-021-81962-6
- Brawand D, Wagner CE, Li YI, Malinsky M, Keller I, Fan S, Simakov O, Ng AY, Lim ZW, Bezaul E, et al. 2014. The genomic substrate for adaptive radiation in African cichlid fish. *Nature* **513**:375–381. doi:10.1038/nature13726
- Carleton K. 2009. Cichlid fish visual systems: mechanisms of spectral tuning. *Integr Zool.* **4**(1):75–86. doi:10.1111/j.1749-4877.2008.00137.x
- Carleton KL, Spady TC, Streelman JT, Kidd MR, McFarland WN, Loew ER. 2008. Visual sensitivities tuned by heterochronic shifts in opsin gene expression. *BMC Biol.* **6**:22–22. doi:10.1186/1741-7007-6-22
- Carroll SB. 2000. Endless forms: the evolution of gene regulation and morphological diversity. *Cell* **101**(6):577–580. doi:10.1016/S0092-8674(00)80868-5
- Carroll SB. 2008. Evo-devo and an expanding evolutionary synthesis: a genetic theory of morphological evolution. *Cell* **134**(1):25–36. doi:10.1016/j.cell.2008.06.030
- Chan YF, Marks ME, Jones FC, Villarreal G, Shapiro MD, Brady SD, Southwick AM, Absher DM, Grimwood J, Schmutz J, et al. 2010. Adaptive evolution of pelvic reduction in sticklebacks by recurrent deletion of a pitxl enhancer. *Science (New York, NY)* **327**(5963):302–305. doi:10.1126/science.1182213
- Earl D, Nguyen N, Hickey G, Harris RS, Fitzgerald S, Beal K, Seledtsov I, Molodtsov V, Raney BJ, Clawson H, et al. 2014. Alignathon: a competitive assessment of whole-genome alignment methods. *Genome Res.* **24**(12):2077–2089. doi:10.1101/gr.174920.114
- El Taher A, Böhne A, Boileau N, Ronco F, Indermaur A, Widmer L, Salzburger W. 2021. Gene expression dynamics during rapid organismal diversification in African cichlid fishes. *Nat Ecol Evol.* **5**(2):243–250. doi:10.1038/s41559-020-01354-3
- Felsenstein J. 1985. Phylogenies and the comparative method. *Am Nat.* **125**(1):1–15. doi:10.1086/284325
- Franchini P, Xiong P, Fruciano C, Meyer A. 2016. The role of microRNAs in the repeated parallel diversification of lineages of Midas cichlid fish from Nicaragua. *Genome Biol Evol.* **8**(5):1543–1555. doi:10.1093/gbe/evw097
- Franchini P, Xiong P, Fruciano C, Schneider RF, Woltering JM, Hulseley CD, Meyer A. 2019. MicroRNA gene regulation in extremely young and parallel adaptive radiations of crater lake cichlid fish. *Mol Biol Evol.* **36**(11):2498–2511. doi:10.1093/molbev/msz168
- Franz M, Lopes CT, Huck G, Dong Y, Sumer O, Bader GD. 2015. Cytoscape.js: a graph theory library for visualisation and analysis. *Bioinformatics* **32**(2):309–311. doi:10.1093/bioinformatics/btv557
- Genner MJ, Seehausen O, Lunt DH, Joyce DA, Shaw PW, Carvalho GR, Turner GF. 2007. Age of cichlids: new dates for ancient lake fish radiations. *Mol Biol Evol.* **24**(5):1269–1282. doi:10.1093/molbev/msm050
- Goenawan IH, Bryan K, Lynn DJ. 2016. Dynet: Visualization and analysis of dynamic molecular interaction networks. *Bioinformatics* **32**(17):2713–2715. doi:10.1093/bioinformatics/btw187
- Grant CE, Bailey TL, Noble WS. 2011. FIMO: scanning for occurrences of a given motif. *Bioinformatics (Oxford, England)* **27**(7):1017–1018. doi:10.1093/bioinformatics/btr064
- Hahn C, Genner MJ, Turner GF, Joyce DA. 2017. The genomic basis of cichlid fish adaptation within the deepwater “twilight zone” of lake malawi. *Evol Lett* **1**(4):184–198. doi:10.1002/evl3.20
- Hofmann CM, O’Quin KE, Marshall NJ, Cronin TW, Seehausen O, Carleton KL, Justin Marshall N. 2009. The eyes have it: regulatory and structural changes both underlie cichlid visual pigment diversity. *PLoS Biol.* **7**(12):e1000266. doi:10.1371/journal.pbio.1000266
- Hu SQ, Liao YF, Zheng J, Gou LN, Regmi A, Zafar MI, Chen LL. 2019. In silico integration approach reveals key microRNAs and their target genes in follicular thyroid carcinoma. *Biomed Res Int.* **2019**:2725192. doi:10.1155/2019/2725192
- Hubisz MJ, Pollard KS, Siepel A. 2011. Phast and rphast: phylogenetic analysis with space/time models. *Briefings Bioinformatics* **12**(1):41–51. doi:10.1093/bib/bbq072
- Hughes LC, Ortí G, Huang Y, Sun Y, Baldwin CC, Thompson AW, Arcila D, Betancur R, Li C, Becker L, et al. 2018. Comprehensive phylogeny of ray-finned fishes (actinopterygii) based on transcriptomic and genomic data. *Proc Natl Acad Sci U S A.* **115**(24):6249–6254. doi:10.1073/pnas.1719358115
- Ichihashi Y, Aguilar-Martinez JA, Farhi M, Chitwood DH, Kumar R, Millon LV, Peng J, Maloof JN, Sinha NR. 2014. Evolutionary developmental transcriptomics reveals a gene network module regulating interspecific diversity in plant leaf shape. *Proc Natl Acad Sci U S A.* **111**(25):2616–2621. doi:10.1073/pnas.1402835111
- Jacob F. 1977. Evolution and tinkering. *Science (New York, NY)* **196**(4295):1161–1166. doi:10.1126/science.860134
- John B, Enright AJ, Aravin A, Tuschl T, Sander C, Marks DS. 2004. Human microRNA targets. *PLoS Biol.* **2**(11):e363. doi:10.1371/journal.pbio.0020363
- Jones FC, Grabherr MG, Chan YF, Russell P, Mauceli E, Johnson J, Swofford R, Pirun M, Zody MC, White S, et al. 2012. The genomic basis of adaptive evolution in threespine sticklebacks. *Nature* **484**(7392):55–61. doi:10.1038/nature10944
- Katoh K, Standley DM. 2013. MAFFT multiple sequence alignment software version 7: improvements in performance and usability. *Mol Biol Evol.* **30**(4):772–780. doi:10.1093/molbev/mst010
- Kautt AF, Kratochwil CF, Nater A, Machado-Schiaffino G, Olave M, Henning F, Torres-Dowdall J, Härer A, Hulseley CD, Franchini P, et al. 2020. Contrasting signatures of genomic divergence during sympatric speciation. *Nature* **588**(7836):106–111. doi:10.1038/s41586-020-2845-0
- Khan A, Fornes O, Stigliani A, Gheorghie M, Castro-Mondragon JA, van der Lee R, Bessy A, Chêneby J, Kulkarni SR, Tan G, et al. 2018. JaspAr 2018: update of the open-access database of transcription factor binding profiles and its web framework. *Nucleic Acids Res.* **46**:D260–D266. doi:10.1093/nar/gkx1126
- King M-C, Wilson AC. 1975. Evolution at two levels in humans and chimpanzees. *Science (New York, NY)* **188**(4184):107–116. doi:10.1126/science.1090005
- Klisch TJ, Souopgui J, Juergens K, Rust B, Pieler T, Henningfeld KA. 2006. Mxi1 is essential for neurogenesis in xenopus and acts by bridging the pan-neural and proneural genes. *Dev Biol.* **292**(2):470–485. doi:10.1016/j.ydbio.2005.12.037
- Kocher TD. 2004. Adaptive evolution and explosive speciation: the cichlid fish model. *Nat Rev Genet.* **5**(4):288–298. doi:10.1038/nrg1316
- Kole C, Brommer B, Nakaya N, Sengupta M, Bonet-Ponce L, Zhao T, Wang C, Li W, He Z, Tomarev S. 2020. Activating transcription factor 3 (atf3) protects retinal ganglion cells and promotes functional preservation after optic nerve crush. *Invest Ophthalmol Visual Sci.* **61**(2):31. doi:10.1167/iovs.61.2.31
- Kozomara A, Griffiths-Jones S. 2014. Mirbase: annotating high confidence microRNAs using deep sequencing data. *Nucleic Acids Res.* **42**:D68–D73. doi:10.1093/nar/gkt1181
- Kratochwil CF, Liang Y, Gerwin J, Woltering JM, Urban S, Henning F, Machado-Schiaffino G, Hulseley CD, Meyer A. 2018. Agouti-related peptide 2 facilitates convergent evolution of stripe patterns across cichlid fish radiations. *Science* **362**(6413):457–460. doi:10.1126/science.aao6809
- Kratochwil CF, Meyer A. 2014. Mapping active promoters by chip-seq profiling of h3k4me3 in cichlid fish - a first step to uncover cis-regulatory elements in ecological model teleosts. *Mol Ecol Resour* **5**:761–771. doi:10.1111/1755-0998.12350

- Kratochwil CF, Meyer A. 2015. Evolution: tinkering within gene regulatory landscapes. *Curr Biol*. **25**(7):R285–R288. doi:10.1016/j.cub.2015.02.051
- Loh Y-HE, Yi SV, Streelman JT. 2011. Evolution of microRNAs and the diversification of species. *Genome Biol Evol*. **3**:55–65. doi:10.1093/gbe/evq085
- Malinsky M, Svardal H, Tyers AM, Miska EA, Genner MJ, Turner GF, Durbin R. 2018. Whole-genome sequences of Malawi cichlids reveal multiple radiations interconnected by gene flow. *Nat Ecol Evol*. **2**(12):1940–1955. doi:10.1038/s41559-018-0717-x
- McGee MD, Borstein SR, Meier JJ, Marques DA, Mwaiko S, Taabu A, Kishe MA, O'Meara B, Bruggmann R, Excoffier L, et al. 2020. The ecological and genomic basis of explosive adaptive radiation. *Nature* **586**(7827):75–79. doi:10.1038/s41586-020-2652-7
- Medina-Rivera A, Defrance M, Sand O, Herrmann C, Castro-Mondragon JA, Delerce J, Jaeger S, Blanchet C, Vincens P, Caron C, et al. 2015. Rsat 2015: regulatory sequence analysis tools. *Nucleic Acids Res*. **43**(W1):W50–W56. doi:10.1093/nar/gkv362
- Mehta TK, Koch C, Nash W, Knaack SA, Sudhakar P, Olbei M, Bastkowski S, Penso-Dolfín L, Korcsmaros T, Haerty W, et al. 2021. Evolution of regulatory networks associated with traits under selection in cichlids. *Genome Biol*. **22**(1):25–25. doi:10.1186/s13059-020-02208-8
- Minchington TG, Griffiths-Jones S, Papalopulu N. 2020. Dynamical gene regulatory networks are tuned by transcriptional autoregulation with microRNA feedback. *Sci Rep*. **10**(1):12960. doi:10.1038/s41598-020-69791-5
- Mullany LE, Herrick JS, Wolff RK, Stevens JR, Samowitz W, Slattery ML. 2018. MicroRNA-transcription factor interactions and their combined effect on target gene expression in colon cancer cases. *Genes Chromosomes Cancer*. **57**(4):192–202. doi:10.1002/gcc.22520
- Nandamuri SP, Conte MA, Carleton KL. 2018. Multiple trans QTL and one cis-regulatory deletion are associated with the differential expression of cone opsins in African cichlids. *BMC Genomics* **19**:945–945. doi:10.1186/s12864-018-5328-z
- Nersisyan S, Galatenko A, Galatenko V, Shkurnikov M, Tonevitsky A. 2021. MiRGTf-net: integrative miRNA-gene-TF network analysis reveals key drivers of breast cancer recurrence. *PLoS One* **16**(4):e0249424. doi:10.1371/journal.pone.0249424
- Nozawa M, Fujimi M, Iwamoto C, Onizuka K, Fukuda N, Ikeo K, Gojobori T. 2016. Evolutionary transitions of microRNA-target pairs. *Genome Biol Evol*. **8**(5):1621–1633. doi:10.1093/gbe/evw092
- O'Quin KE, Hofmann CM, Hofmann HA, Carleton KL. 2010. Parallel evolution of opsin gene expression in African cichlid fishes. *Mol Biol Evol*. **27**(12):2839–2854. doi:10.1093/molbev/msq171
- O'Quin KE, Schulte JE, Patel Z, Kahn N, Naseer Z, Wang H, Conte MA, Carleton KL. 2012. Evolution of cichlid vision via trans-regulatory divergence. *BMC Evol Biol*. **12**(1):251. doi:10.1186/1471-2148-12-251
- O'Quin KE, Smith D, Naseer Z, Schulte J, Engel SD, Loh Y-HHE, Streelman JT, Boore JL, Carleton KL. 2011. Divergence in cis-regulatory sequences surrounding the opsin gene arrays of African cichlid fishes. *BMC Evol Biol*. **11**(1):120. doi:10.1186/1471-2148-11-120
- Peter IS, Davidson EH. 2011. Evolution of gene regulatory networks controlling body plan development. *Cell* **144**(6):970–985. doi:10.1016/j.cell.2011.02.017
- Plaisier CL, O'Brien S, Bernard B, Reynolds S, Simon Z, Toledo CM, Ding Y, Reiss DJ, Paddison PJ, Baliga NS. 2016. Causal mechanistic regulatory network for glioblastoma deciphered using systems genetics network analysis. *Cell Syst*. **3**(2):172–186. doi:10.1016/j.cels.2016.06.006
- Pollard KS, Hubisz MJ, Rosenbloom KR, Siepel A. 2010. Detection of nonneutral substitution rates on mammalian phylogenies. *Genome Res*. **20**(1):110–121. doi:10.1101/gr.097857.109
- Prager EM, Wilson AC. 1975. Slow evolutionary loss of the potential for interspecific hybridization in birds: a manifestation of slow regulatory evolution. *Proc Natl Acad Sci U S A*. **72**(1):200–204. doi:10.1073/pnas.72.1.200
- Puntambekar S, Newhouse R, San-Miguel J, Chauhan R, Vernaz G, Willis T, Wayland MT, Umrana Y, Miska EA, Prabhakaran S. 2020. Evolutionary divergence of novel open reading frames in cichlids speciation. *Sci Rep*. **10**(1):21570. doi:10.1038/s41598-020-78555-0
- Quinlan AR, Hall IM. 2010. Bedtools: a flexible suite of utilities for comparing genomic features. *Bioinformatics* **26**(6):841–842. doi:10.1093/bioinformatics/btq033
- Remenyi J, van den Bosch MWM, Palygin O, Mistry RB, McKenzie C, Macdonald A, Hutvagner G, Arthur JSC, Frenguelli BG, Pankratov Y. 2013. Mir-132/212 knockout mice reveal roles for these miRNAs in regulating cortical synaptic transmission and plasticity. *PLoS One* **8**(4):e62509. doi:10.1371/journal.pone.0062509
- Riffo-Campos ÁL, Riquelme I, Brebi-Mieville P. 2016. Tools for sequence-based miRNA target prediction: what to choose? *Int J Mol Sci*. **17**(12):1987. doi:10.3390/ijms17121987
- Ronco F, Matschner M, Böhne A, Boila A, Büscher HH, El Taher A, Indermaur A, Malinsky M, Ricci V, Kahmen A, et al. 2021. Drivers and dynamics of a massive adaptive radiation in cichlid fishes. *Nature* **589**(7840):76–81. doi:10.1038/s41586-020-2930-4
- Salzburger W. 2018. Understanding explosive diversification through cichlid fish genomics. *Nat Rev Genet*. **19**:705–717. doi:10.1038/s41576-018-0043-9
- Sandkam BA, Campello L, O'Brien C, Nandamuri SP, Gammerdinger W, Conte M, Swaroop A, Carleton KL. 2020. Tbx2a modulates switching of RH2 and LWS opsin gene expression. *Mol Biol Evol*. **37**(7):2002–2014. doi:10.1093/molbev/msaa062
- Santos ME, Braasch I, Boileau N, Meyer BS, Sauteur L, Böhne A, Belting H-G, Affolter M, Salzburger W, Santos E, et al. 2014. The evolution of cichlid fish egg-spots is linked with a cis-regulatory change. *Nat Commun*. **5**(1):5149. doi:10.1038/ncomms6149
- Sayed M, Park JW. 2020. Miringo: prediction of biological processes indirectly targeted by human microRNAs. *bioRxiv* 2020.2007.2024.220335.
- Sharma R, Upadhyay S, Bhat B, Singh G, Bhattacharya S, Singh A. 2020. Abiotic stress induced miRNA-TF-gene regulatory network: a structural perspective. *Genomics* **112**(1):412–422. doi:10.1016/j.ygeno.2019.03.004
- Sharma R, Upadhyay S, Bhattacharya S, Singh A. 2021. Abiotic stress-responsive miRNA and transcription factor-mediated gene regulatory network in *Oryza sativa*: construction and structural measure study. *Front Genet*. **12**:618089. doi:10.3389/fgene.2021.618089
- Simkin AT, Bailey JA, Gao F-B, Jensen JD. 2014. Inferring the evolutionary history of primate microRNA binding sites: overcoming motif counting biases. *Mol Biol Evol*. **31**(7):1894–1901. doi:10.1093/molbev/msu129
- Simkin A, Geissler R, McIntyre ABR, Grimson A. 2020. Evolutionary dynamics of microRNA target sites across vertebrate evolution. *PLoS Genet*. **16**(2):e1008285. doi:10.1371/journal.pgen.1008285
- Stergachis AB, Neph S, Sandstrom R, Haugen E, Reynolds AP, Zhang M, Byron R, Canfield T, Stelting-Sun S, Lee K, et al. 2014. Conservation of trans-acting circuitry during mammalian regulatory evolution. *Nature* **515**(7527):365–370. doi:10.1038/nature13972
- Thompson D, Regev A, Roy S. 2015. Comparative analysis of gene regulatory networks: from network reconstruction to evolution. *Annu Rev Cell Dev Biol*. **31**:399–428. doi:10.1146/annurev-cellbio-100913-012908
- Thompson DA, Roy S, Chan M, Styczynski MP, Pfiffner J, French C, Socha A, Thielke A, Napolitano S, Muller P, et al. 2013. Evolutionary principles of modular gene regulation in yeasts. *eLife* **2**:e00603. doi:10.7554/eLife.00603
- Vernaz G, Malinsky M, Svardal H, Du M, Tyers AM, Santos ME, Durbin R, Genner MJ, Turner GF, Miska EA. 2021. Mapping epigenetic divergence in the massive radiation of Lake Malawi cichlid fishes. *Nat Commun*. **12**(1):5870. doi:10.1038/s41467-021-26166-2

- Wagner CE, Harmon LJ, Seehausen O. 2012. Ecological opportunity and sexual selection together predict adaptive radiation. *Nature* **487**(7407):366–369. doi:10.1038/nature11144
- Warnefors M, Mossinger K, Halbert J, Studer T, VandeBerg JL, Lindgren I, Fallahshahroudi A, Jensen P, Kaessmann H. 2017. Sex-biased microRNA expression in mammals and birds reveals underlying regulatory mechanisms and a role in dosage compensation. *Genome Res.* **27**(12):1961–1973. doi:10.1101/gr.225391.117
- Wilson AC, Maxson LR, Sarich VM. 1974. Two types of molecular evolution: evidence from studies of interspecific hybridization. *Proc Natl Acad Sci U S A.* **71**(7):2843–2847. doi:10.1073/pnas.71.7.2843
- Wittkopp PJ, Haerum BK, Clark AG. 2008. Regulatory changes underlying expression differences within and between drosophila species. *Nat Genet.* **40**(3):346–350. doi:10.1038/ng.77
- Xiong P, Hulsey CD, Meyer A, Franchini P. 2018. Evolutionary divergence of 3' UTRs in cichlid fishes. *BMC Genomics* **19**(1):433. doi:10.1186/s12864-018-4821-8
- Xiong P, Schneider RF, Hulsey CD, Meyer A, Franchini P. 2019. Conservation and novelty in the microRNA genomic landscape of hyperdiverse cichlid fishes. *Sci Rep.* **9**(1):13848. doi:10.1038/s41598-019-50124-0
- Yanai I, Hunter CP. 2009. Comparison of diverse developmental transcriptomes reveals that coexpression of gene neighbors is not evolutionarily conserved. *Genome Res.* **19**(12):2214–2220. doi:10.1101/gr.093815.109
- You G, Zu B, Wang B, Fu Q, Li F. 2020. Identification of miRNA–mRNA–TF regulatory network and crucial pathways involved in tetralogy of fallot. *Front Genet.* **11**:552. doi:10.3389/fgene.2020.00552